ISSUE 37 DECEMBER 2023

GAṆANAM (गणनम्)

HIGH PERFORMANCE *COMPUTING* NEWSLETTER

INSTITUTE FOR PLASMA RESEARCH, INDIA

INSIDE THIS ISSUE
(3 Pages)

Generation of a nearly mono-energetic weakly relativistic electron beam from laser-cluster interaction with an ambient magnetic field

Kalyani Swain (PhD Student, Basic Theory and Simulation Division, IPR)
Email: kalyani.swain@ipr.res.in

*F*or the last few decades, table-top laser-plasma accelerators have brought significant progress to replace traditional high-energy accelerators. The production of a relativistic electron beam (REB) from laser-plasma interaction has also become a recent topic of interest in the laser plasma community as REB has wide applications in the fast ignition technique of inertial confinement fusion and many medical applications.

In one of our recent studies [1] on laser interaction (for a wavelength of 800nm and intensity greater than 10^{16}W/cm^2) with a deuterium nanocluster (size=2.2nm) in an ambient magnetic field B_0 demonstrate that collisionless absorption of laser light occurs in two stages via anharmonic resonance and electron-cyclotron resonance (ECR) or relativistic ECR (RECR) processes. Using a rigid sphere model (RSM) and particle-in-cell (PIC) simulation, we show that the auxiliary magnetic field B_0 enhances the coupling of the laser field to cluster electrons via improved frequency matching for ECR or RECR as well as phase matching for the prolonged duration of the 5-fs (FWHM) broadband pulse. As a result, the average absorbed energy per electron ε significantly jumps up to ~36–70 times its ponderomotive energy (U_p) for laser intensity I_0=7.13×10^{16} W/cm^2 (see Fig.1).

Now, to understand the dynamics of these energetic electrons towards the formation of an electron beam, the energy and angular distributions of these electrons have been thoroughly analysed. In Fig.2 we show the energy distribution of PIC electrons at three points B_0 ≈ 0.35ω, ω, 1.25ω corresponding to point A, B and C of Fig.1. With a low value B_0 (or without it, point A), more electrons (yellow region) are near lower energy $\overline{\mathcal{E}_A}$≈ 0.1; however, the energy tail with a few electrons extends up to $\overline{\mathcal{E}_A}$≈ 2.6. This is the typical energy distribution of electrons one mostly finds in the case of Interaction LCI (Laser Cluster Interaction) with a very low B_0 (or without B_0). On the other hand, for higher B_0 values corresponding to B and C, more electrons are pushed around $\overline{\mathcal{E}_A}$ ≈ 36 and $\overline{\mathcal{E}_A}$ ≈ 68. This highlights the nearly monoenergetic nature of the electrons in LCI with an ambient magnetic field.

Angular deflection of an electron (θ_r) in the position space is defined as the angle between the laser light propagation in the z direction (the direction of B_{ext} = $B_0\hat{Z}$) and its position vector r. This elevation angle can be obtained from z = r cosθ_r , r⊥ = r sinθ_r; where r⊥ = $\sqrt{x^2+y^2}$. Fig.3 shows histograms of electrons versus θ_r (left column) and respective polar plots (right column) with their normalized position r/R_0 vs θ_r corresponding to those energy spectra in (A, B, C) Fig.2. For lower B_0 = 0.35ω (point A of Fig.2), electrons are spread over a wide angular range θ_r ≈ 0–175° (Fig.3.a1) and the distribution in the (r, θ_r) plane explains that the angular spread contains only low-energy electrons (Fig.3.a2) due to the weak coupling of the laser light to the cluster electrons. However, for B_0 = ω, 1.25ω (point B and C of Fig.2), the angular spread of electrons are $\Delta\theta_r$< 4°-3° (Fig.3.b1,c1) and these electrons propagate at r ≈ 375R_0, 500R_0 by aligning themselves more towards the magnetic-field direction z like a narrow cone. This demonstrates that the ambient magnetic field near ECR or RECR probes the ejected electrons to form a narrow conical beam gyrating about the z axis as well as propagating in the z direction in the position space like a spiral.

Position coordinates (r, θ_r) of electrons are important to know how far these electrons have been transported as a beam and at what orientation. However, momentum coordinates (p, θ_p) is often more physically relevant to determine the transport properties of electrons and the kind of magnetic configuration required to transport these electrons as a beam. θ_p can also be calculated in a similar way like θ_r, from p_z = p cosθ_p and p⊥ = p sinθ_p, where p⊥ =$\sqrt{p_x^2+p_y^2}$ .From the histograms of electrons and respective polar plots with their normalized momentum p/c vs θ_p (results are not shown here; see the details in [2]) corresponding to those energy spectra in (point B, C) Fig.2 shows that the momentum of beam electrons reaches weakly relativistic values p = $\sqrt{p_\perp^2+p_y^2}$ ≈ 0.875c, 1.25c for B_0=0.057,0.07. All electrons gyrate around the surface of the cone with wide opening angle at an angular spread of $\Delta\theta_p$ < 5° which spirally propagate in the z direction with increasing energy [2]

Furthermore, with increasing cluster size from 2.2nm to 3.3nm and 4.4nm, the electron beam becomes more intense with greater number of energetic electrons. Note that, a higher intensity I_0=1.83×10^{17} W/cm^2 is required while considering the bigger clusters to ensure 100% outer-ionisation of the cluster electrons. In Fig.4 we show the polar plots of the normalized position r/R_0 vs θ_r for the electrons corresponding to B0 = 0.057,0.078 (column wise) for the above mentioned cluster sizes. The angular spread ($\Delta\theta_r$~3°) with narrow opening angle along z-direction is the same for all cluster sizes.

The PIC simulation results show a close matching with RSM results (a detail explanation is given in Ref.[2]). Here, we use an in-house developed 3D electrostatic PIC code [3] which is upgraded to hybrid-PIC [2] for this particular work. This serial code takes ~35 mins for the smaller cluster size (2.2 nm) for single value of B0 in one CPU node of ANTYA-HPC facility at IPR. However, for bigger cluster sizes (3.3nm and 4.4nm) the run time is nearly 4.5hours. Also, to generate Fig.1 we need to scan ~ 50-60 B0 values and the corresponding time data of individual particles for all other Figures. Through message passing interface (MPI) we manage to use 40 nodes of ANTYA at a single run which has greatly reduced the total computation time.

> ***Electrons generated from the laser cluster interaction in an ambient magnetic field at electron cyclotron resonance (ECR) or relativistic ECR (RECR) can emerge as a nearly mono energetic weakly relativistic conical spiral electron beam with an angular spread Δθr~3°***

References:

1. K. Swain, S. S. Mahalik, and M. Kundu, Sci. Rep. 12, 11256 (2022)
2. K. Swain, S. S. Mahalik, and M. Kundu, PHYSICAL REVIEW A 108, 053104 (2023).
3. M. Kundu and D. Bauer, Phys. Rev. Lett. 96, 123401 (2006).

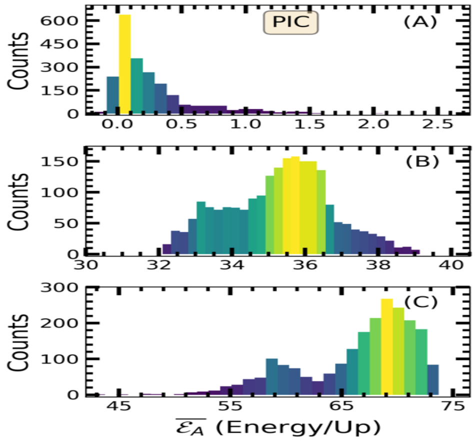

Figure 2 Energy distribution of ejected electrons from the deuterium cluster corresponding to the ambient magnetic fields B_0 ≈ 0.02, 0.057, 0.07 a.u. (at A, B, and C in Fig. 1). The color coding is over the electron count and the yellow (light gray) region highlights maximum electron counts and respective energies $\overline{\mathcal{E}_A}$.

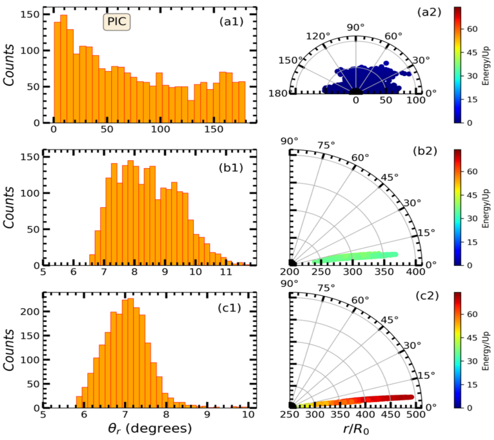

Figure 3 Histograms showing the distributions of angular deflection θr of electrons (left column) and respective polar plots (right column) with their normalized position r/R0 vs θr corresponding to those energy spectra in Figs. 2(a)–2(c) for B_0 =0.02, 0.057, 0.07 a.u., respectively. Polar coordinates (r, θ_r) are color coded with their energy normalized by U_p.

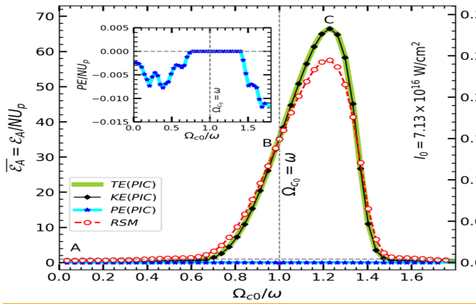

Figure 1 The average total energy ($\overline{\mathcal{E}_A}$), kinetic energy (KE), and potential energy (PE) per cluster electron are plotted vs normalized electron-cyclotron frequency $_c$/ω for a range of ambient field B_0 ≈ 0–2ω with an n = 5 cycle pulse of I_0 ≈ 7.13 × 10^{16} W/cm^2 irradiating a deuterium cluster of N = 2176 and R_0 = 2.2 nm.

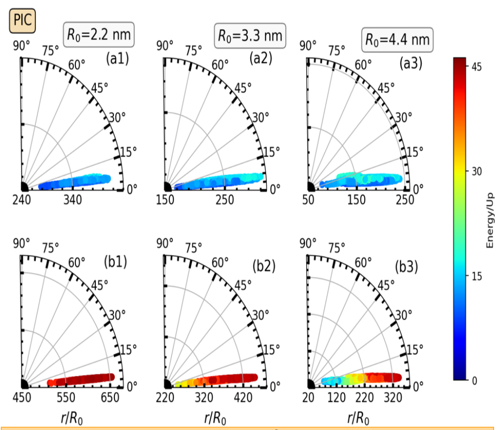

Figure 4 The angular distribution of lectrons is shown in the (r, θ_r) planes corresponding to B_0=0.057,0.078. Polar coordinates (r, θ_r) of electrons are color coded with their energy normalized by U_p.

Profiling 2D matrix multiplication code: Comparison Study between Serial and Parallel approach using Intel VTune Profiler

Intel VTune Profiler can be used for profiling codes written in C/C++ and Fortran languages. The performance statistics data collected from the profiler can enable users to identify and fix performance issues quickly, reducing development time and improving overall code performance and system efficiency. For more details, you may visit the Intel VTune Official Documentation here. Steps to configure Intel VTune Profiler on ANTYA can be found in *GAṆANAM* Issue 28 here.

This article focuses on analysing the programming approach's influence on matrix multiplication performance, a fundamental mathematical operation with widespread applications in computational sciences. For this comparative study, we have selected a matrix multiplication of size 512*512 written in the C language with both serial and parallel programming approaches. All source and output files are accessible on GitHub here.

There are several analysis areas included with Intel VTune, including parallelism, micro-architecture, algorithms, and platform analysis. Parallelism and algorithms, which deal with threading, hotspot analysis, and memory usage, are the two most often utilized analysis categories. Threading and memory usage analysis are employed in the comparison study.

Case 1: Threading analysis using VTune Profiler

The comparative analysis indicated that by distributing the jobs, the parallel programming strategy reduced the elapsed time by 65% and increased the effective CPU utilisation to 10% from 2.5%.

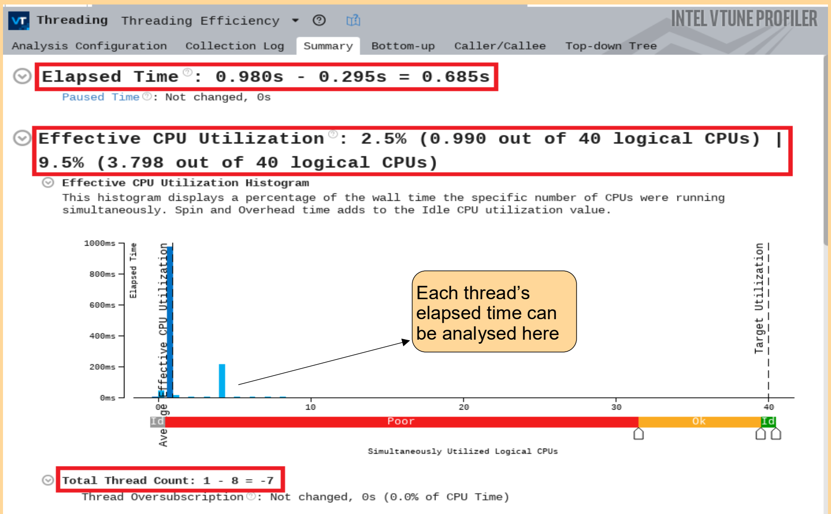

Case 2: Memory Consumption Analysis using VTune Profiler

According to the comparison study, the parallel programming approach uses around ten times more memory than the serial approach. The cause is the generation of new threads or processes.

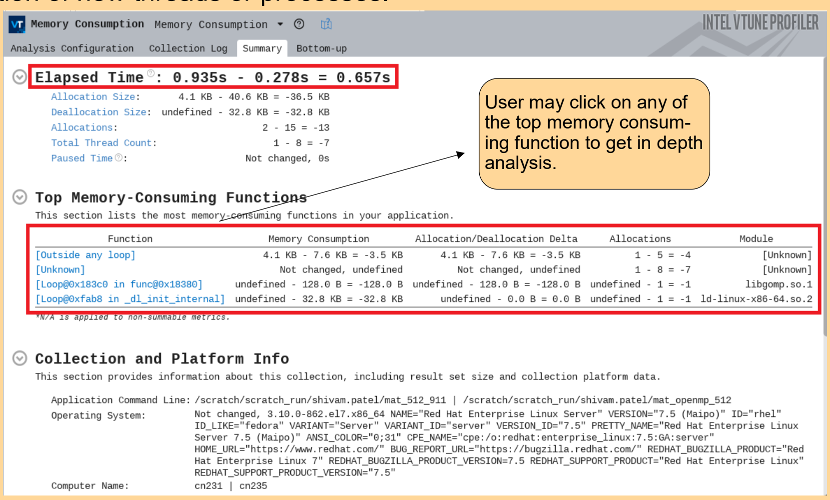

ANTYA UPDATES AND NEWS

1. New Packages/Applications Installed

Modules list remains the same for this month. To check the list of available modules:
$ module avail –l

HPC PICTURE OF THE MONTH

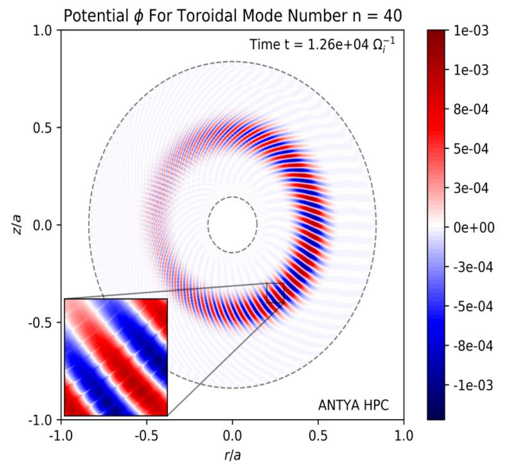

Pic Credit: Gopal Mailapalli

Ion Temperature Gradient (ITG) modes are drift type modes driven unstable if the gradient in temperature is more than the gradient in plasma density in Tokamaks. The phase velocity of the mode is in the ion diamagnetic direction, which is counter-clockwise in the figure, which shows 2D eigenmode structures of an ITG mode. The streaks (sharp features) as shown in the inset plot indicates the effect of kinetic or non-adiabatic electrons.

The plot is generated using **Global Gyrokinetic - PIC code ORB5** in collaboration with EPFL, Switzerland. **This simulation is run for a grid resolution of 512 x 512 x 256, with 640 Million gyrokinetic ions and drift kinetic electrons each, which took 6 days on 1024 cores (32 nodes x 32 cores per node)**. The geometry and equilibrium considered in the simulation, closely resembles the DIII-D tokamak and the cross-section is taken at toroidal angle zero.

TIP OF THE MONTH

The latest version of MATLAB-2023b (Update 4) has been installed on the Visualization node of ANTYA Cluster. For usage, a user has to load this MATLAB module by using the following command.

```
[user@visualization ~]$ module load MATLAB/2023bu4
```

ANTYA Utilization: NOVEMBER 2023

ANTYA Daily Observed Workload

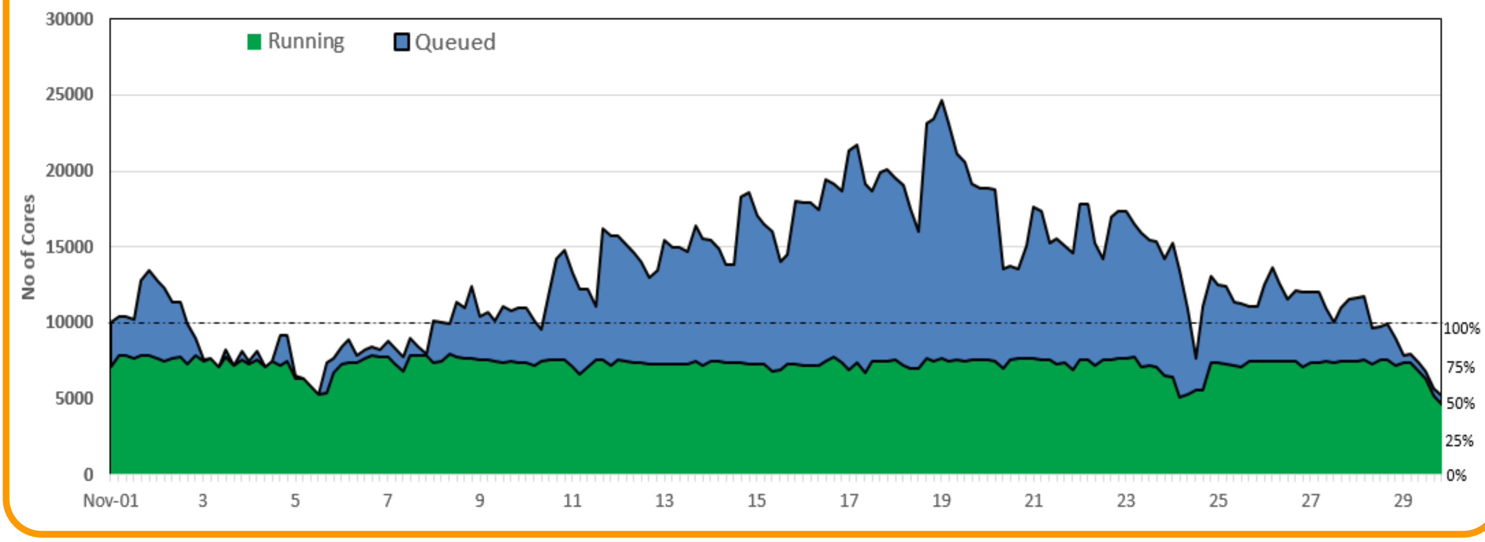

Other Recent Work on HPC (Available in IPR Library)

Optimization of Tritium Losses Due to Ion Beam Interaction for DT Neutron Production by Binary Collision Approximation Method	**Varun Vijay Savadi**
First operation of LLMHD loop with electromagnet for R & D MHD experiments	**Anita Patel**
Fully kinetic electrostatic Particle in Cell simulations using open-source 3D solver for space thruster application	**Sneha Gupta**
Magnetic Island Coalescence Driven Reconnection and Role of Shear flows	**Jagannath Maha-patra**
Effect of Electrons and Ions Mobility on Edge Biasing in Toka-mak Plasmas	**Vijay Shankar**
Physics and Engineering Considerations for Compact Fusion Pilot Plants	**Shishir Deshpande**
Beam driven electromagnetic instability in high temperature plasma	**Anjan Kumar Paul**
Study of ELMs in presence of Stably Operating Coherent Modes	**Kaushalkumar Parikha**
Excitation of fore wake structures in a flowing dusty plasma	**Krishan Kumar**
Inverse Cascade in a 3D Stably Stratified 3D Yukawa Liquid Subjected Plane Couette Flow	**Suruj Jyoti Kalita**
Roration/Spin of Plasma BLOB in Edge AND Scrape off Layer Regions	**Nirmal K. Bisai**

ANTYA HPC USERS' STATISTICS— NOVEMBER 2023

- **Total Successful Jobs~ 1867**
- **Top Users** (Cumulative Resources)
  - **CPU Cores** — **Amit Singh**
  - **GPU Cards** — **Shishir Biswas**
  - **Walltime** — **Vinod Saini**
  - **Jobs** — **Jugal Chowdhury**

Acknowledgement

The HPC Team, Computer Division IPR, would like to thank all Contributors for the current issue of *GAṆANAM*.

On Demand Online Tutorial Session on HPC Environment for New Users Available
Please send your request to ***hpcteam@ipr.res.in.***

Join the HPC Users Community
hpcusers@ipr.res.in
If you wish to contribute an article in GAṆANAM, please write to us.

Contact us
HPC Team
Computer Division, IPR
Email: ***hpcteam@ipr.res.in***